Cell Reports, Volume *43*

Supplemental information

GABA co-released from striatal dopamine axons dampens phasic dopamine release through autoregulatory $GABA_A$ receptors

Jyoti C. Patel, Ang D. Sherpa, Riccardo Melani, Paul Witkovsky, Madeline R. Wiseman, Brian O'Neill, Chiye Aoki, Nicolas X. Tritsch, and Margaret E. Rice

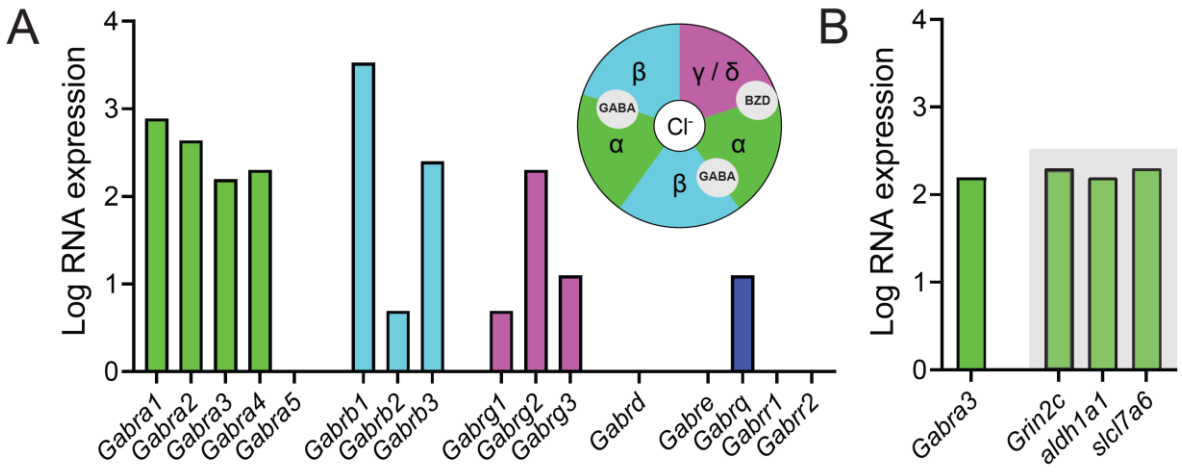

Figure S1. Dopamine neurons possess mRNA encoding multiple $GABA_AR$ subunits (Related to Main Figure 1).

(A) Analysis using DropViz of mRNA levels for genes encoding various $GABA_AR$ subunits in tyrosine hydroxylase (TH) containing midbrain DA neurons along with a Cartoon showing the top view of the pentameric organization of a $GABA_AR$ with alpha (α), beta (β), and gamma/delta (γ/δ) subunits surrounding a central Cl^- pore; GABA and benzodiazepine (BZD) binding sites are also shown.

(B) Analysis using DropViz showing similar mRNA expression levels for the *Gabra3* gene encoding α3-$GABA_AR$ subunits across subclusters of TH-positive cells including those expressing *Grin2c* which encodes NMDAR2c primarily located in a subset of SNc DA neurons,[S1] TH neurons expressing *aldh1a1* which encodes ALDH1a1 and primarily located in the ventral tier of SNc,[S1,S2] and TH neurons expressing *Slc17a6* which encodes the vesicular glutamate transporter, vGluT2, and is primarily located in the VTA and lateral SNc.[S2,S3]

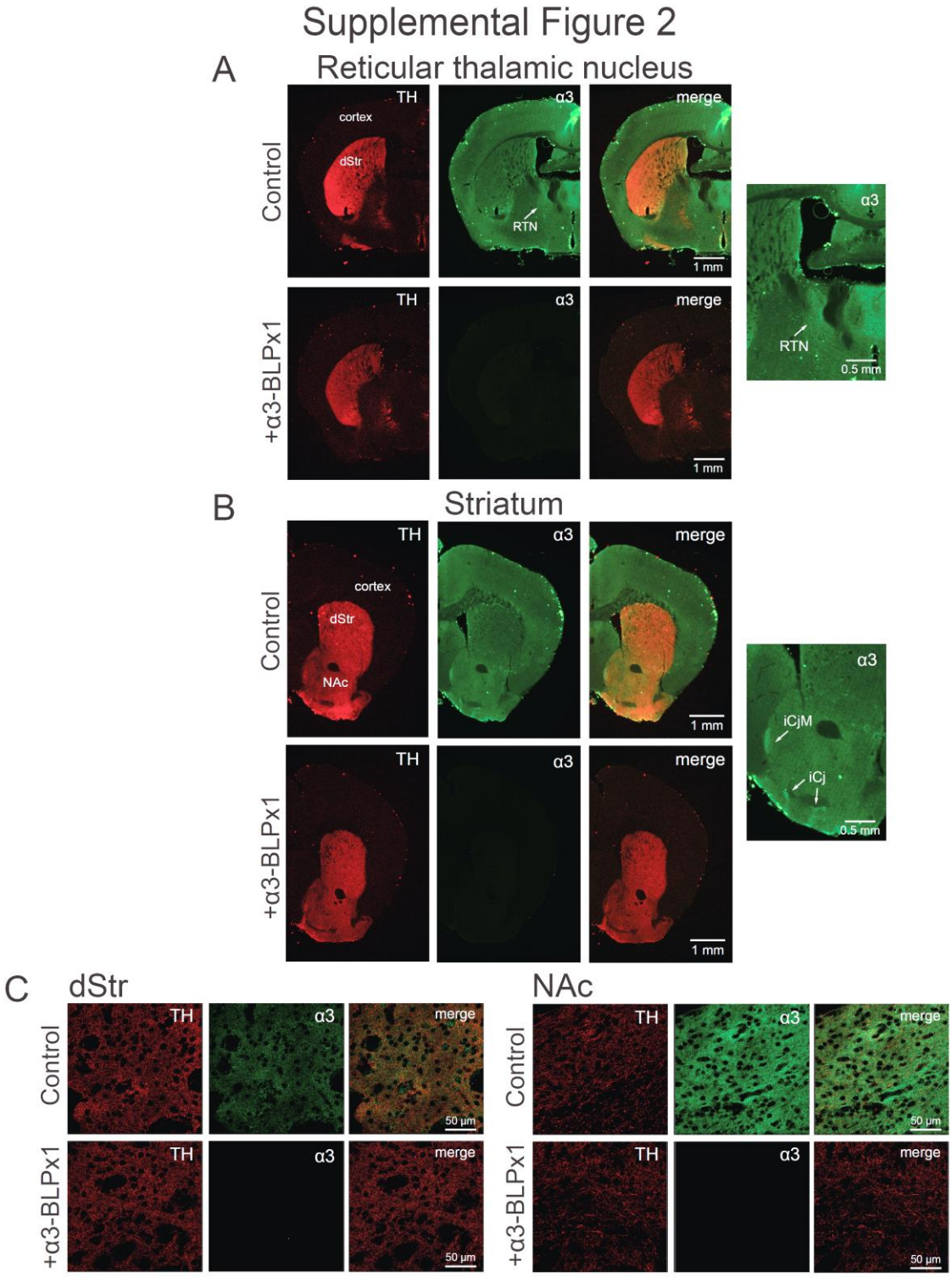

Supplemental Figure 2. Immunohistochemistry showing fluorescence staining for α3-GABA$_A$R subunits in reticular thalamic nucleus and striatum (Related to Main Figure 1).

(A) Representative coronal sections containing the posterior striatum immunolabeled with an anti-tyrosine hydroxylase (TH) antibody (red) for DA axons, as well as the reticular thalamic nucleus (RTN) labeled with an anti-α3-subunit antibody (green) in the absence and presence of preadsorption with its corresponding blocking peptide (BLPx1). Scale bars, 1 mm. Enlarged image on the right shows high labeling of α3 in the RTN, thereby providing evidence that the α3-subunit selective antibody used produces the expected pattern of immunolabeling seen in other studies. Scale bar, 0.5 mm.

(B) Representative coronal striatal sections immunolabeled with TH for DA axons as well as an antibody against α3-$GABA_AR$ subunits with and without preadsorption with its corresponding blocking peptide (BLPx1). Scale bars, 1 mm. Enlarged image on the right shows stronger labeling in the islands of Calleja (iCj) and the major island of Calleja (iCjM) *versus* striatum demonstrating the expected pattern of immunolabeling seen in other studies. Scale bar, 0.5 mm.

(C) Representative high magnification confocal images obtained for TH and α3 immunolabeling in the dorsal striatum (dStr) and nucleus accumbens (NAc). In both the RTN and striatal sections fluorescence labeling for α3-$GABA_AR$ subunits was completely absent after preadsorption with its immunogenic blocking peptide. Scale bars, 50 µm.

Images in **A** and **B** were obtained using epifluorescence at 2x (0.06 NA); confocal images in **C** were taken at 60x (1.4 NA).

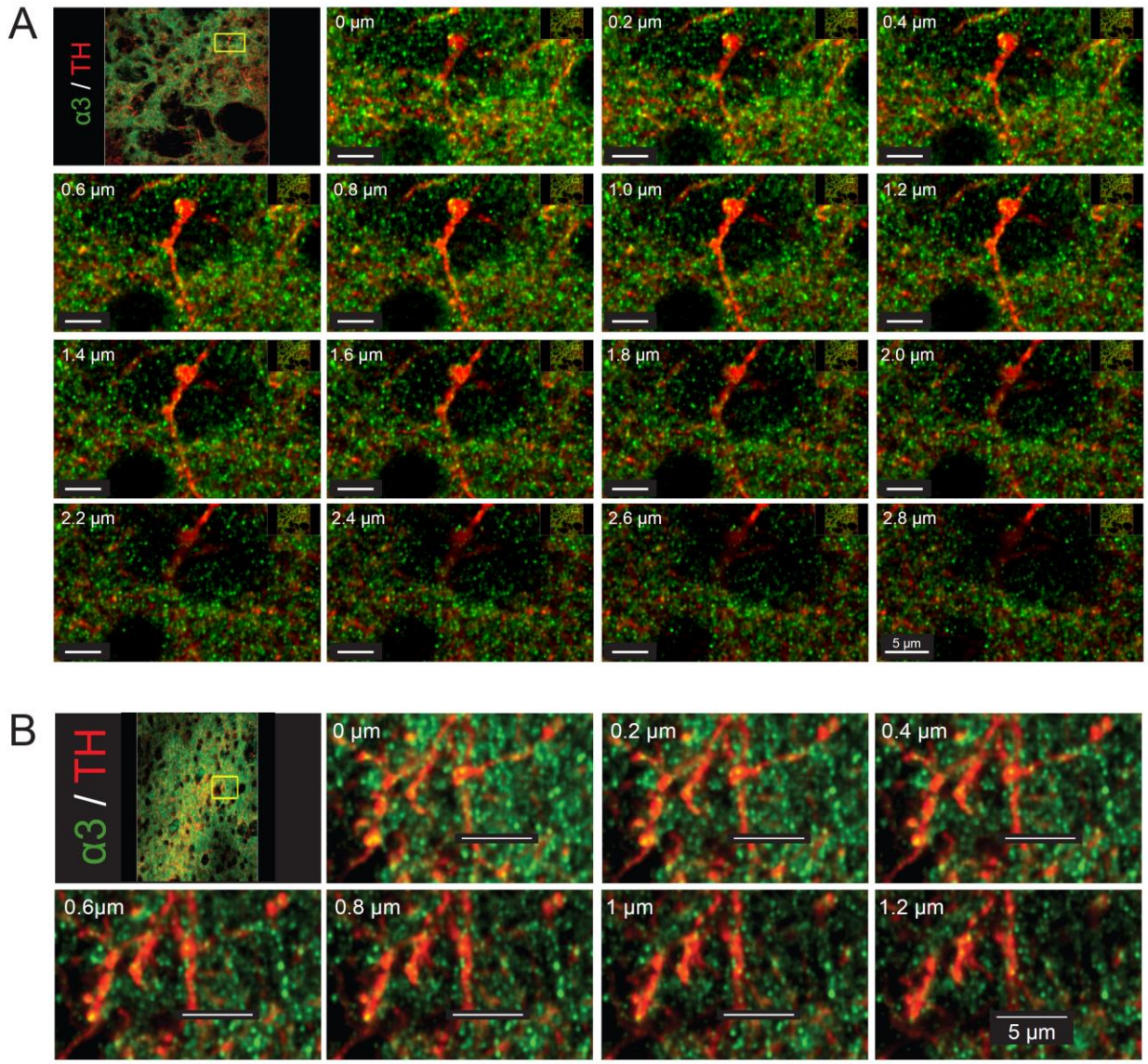

Figure S3. Confocal z-stack images showing colocalization of α3-GABA$_A$R subunits in striatal DA axonal profiles (Related to Main Figure 1).

(A) z-stack of immunohistochemical image of dStr from Figure 1A demonstrating colocalization (yellow puncta) of α3-subunits in DA axonal profiles labeled with an anti-tyrosine hydroxylase (TH) antibody (red). Scale bars, 5 µm.

(B) Another example of a z-stack in the striatum showing the presence of α3-immunoreactive puncta in DA axonal profiles. Scale bars, 5 µm.

Images are shown at successive 0.2 µm intervals taken using confocal at 60x (1.4 NA).

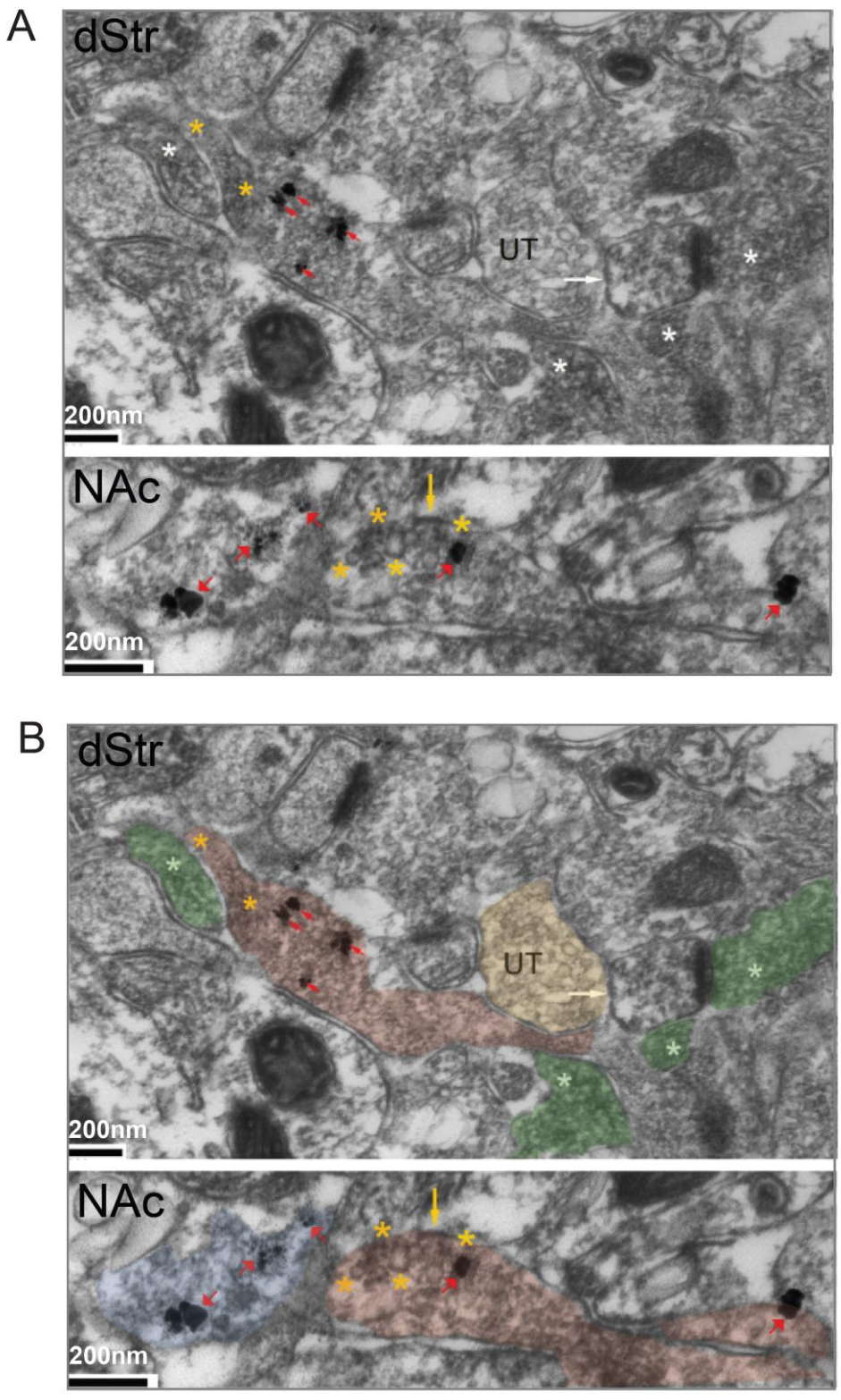

Figure S4. Immuno-electron microscopy showing localization of α3-GABA$_A$R subunits in striatal DA axons (Related to Main Figure 1).

(A) Electronmicrographs from Figure 1B without overlapping color, showing α3-$GABA_AR$ subunits colocalized with TH labeled DA axons in dStr and NAc core. Top panel: TH axons in dStr were identified by the presence of more than one SIG particle within an axonal profile packed with multiple vesicles, such as the one shown (red arrows), while presence of α3-$GABA_AR$ subunits was identified by electron-dense diffuse HRP-DAB labeling of vesicular and plasma membranes (asterisks). α3 subunits within TH axons are highlighted by yellow asterisks, whereas α3-$GABA_AR$ subunits in non-TH axons are highlighted by white asterisks; UT shows an unlabeled axon terminal. The white arrow points to the plasma membrane of a non-TH profile, identifiable as a dendritic spine receiving excitatory synaptic input from a non-TH axon terminal (right-most asterisk), presumably glutamatergic and α3-positive. Scale bar, 200 nm. Bottom panel: TH axons in NAc core were identified as above, and indicated here using the same symbols and shown at a higher magnification to highlight immunolabeling of the plasma membrane of a dually labeled axon (yellow arrow) and of vesicle membranes (encircled by yellow asterisks). Scale bar, 200 nm.

(B) Identical images to those shown in **A** with red overlay highlighting TH-labeled DA axons containing α3 subunits, green overlay highlighting TH negative axons with α3 subunits, blue overlay highlighting TH positive axons without α3 subunits and yellow overlay highlighting an unlabeled axon terminal (UT). Scale bars, 200 nm.

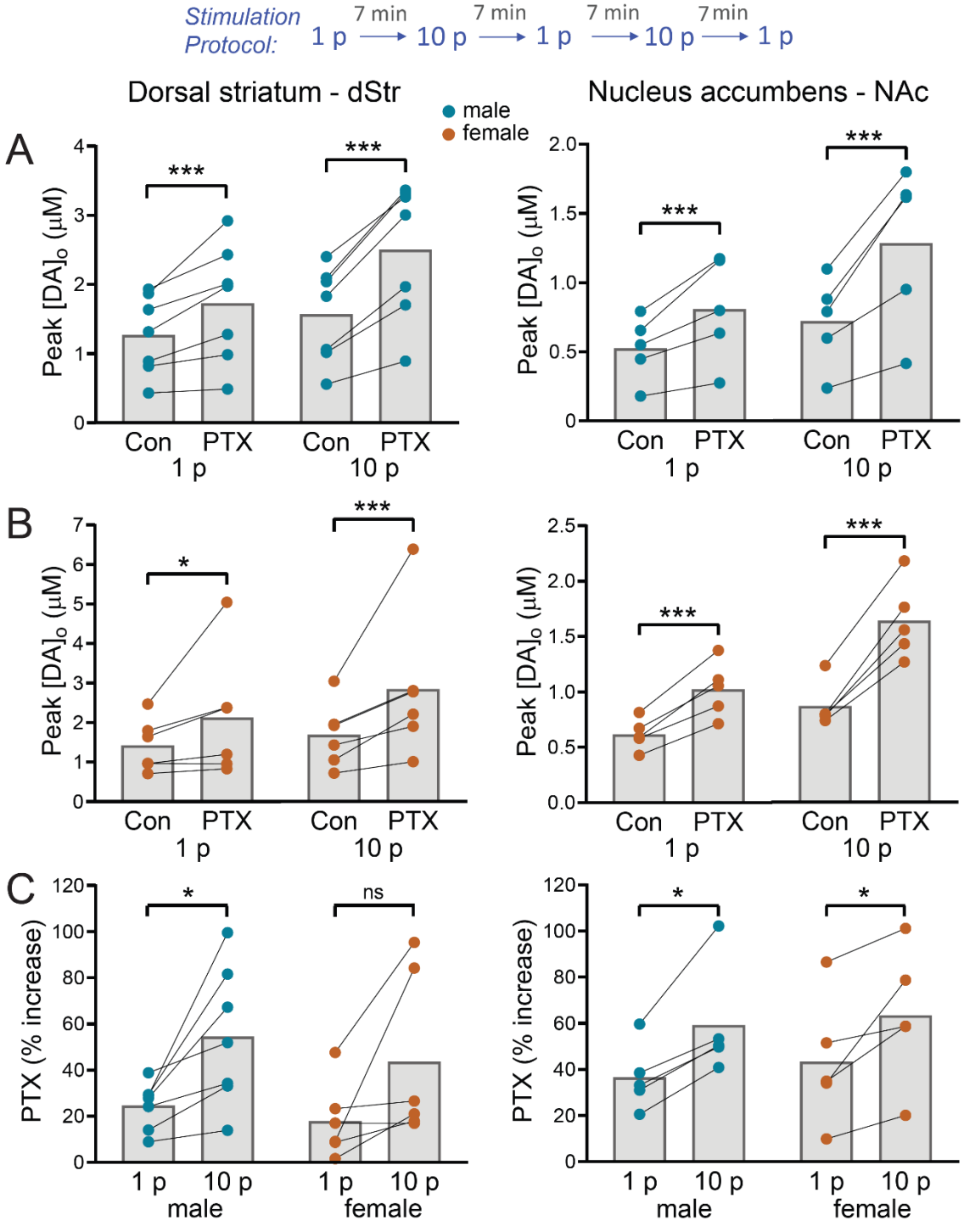

Figure S5. GABA$_A$R regulation of DA release by ambient GABA and endogenously evoked GABA corelease from DA axons in males and females (Related to Main Figures 2, 3 and 4).

(A) Using an alternating stimulation protocol (paired protocol), the $GABA_AR$ Cl^- channel blocker picrotoxin (100 µM, PTX) increased peak $[DA]_o$ evoked by single-pulse (1 p) and multiple-pulse (10 p at 10 Hz) optical stimulation of DA axons in males (blue circles) in both the dStr (n = 7 mice) and NAc (n = 5 mice), thereby supporting both an ambient source and an additional source of GABA from DA axons for DA release regulation.

(B) Similarly, in females (orange circles) PTX significantly increased peak $[DA]_o$ evoked by both 1 p and 10 p in the dStr (n = 6 mice) and NAc (n = 5 mice).

(C) In males, PTX-induced increases in peak $[DA]_o$ were significantly greater when evoked by 10 p than 1 p the dStr and NAc. In females, however, PTX induced greater increases in peak $[DA]_o$ with 10 p than with 1 p in NAc, but not in the dStr.

ns is non-significant $p > 0.05$; *$p < 0.05$; **$p < 0.01$; ***$p < 0.001$ ratio paired t-tests *versus* respective control or paired t-test *versus* respective 1 p stimulation.

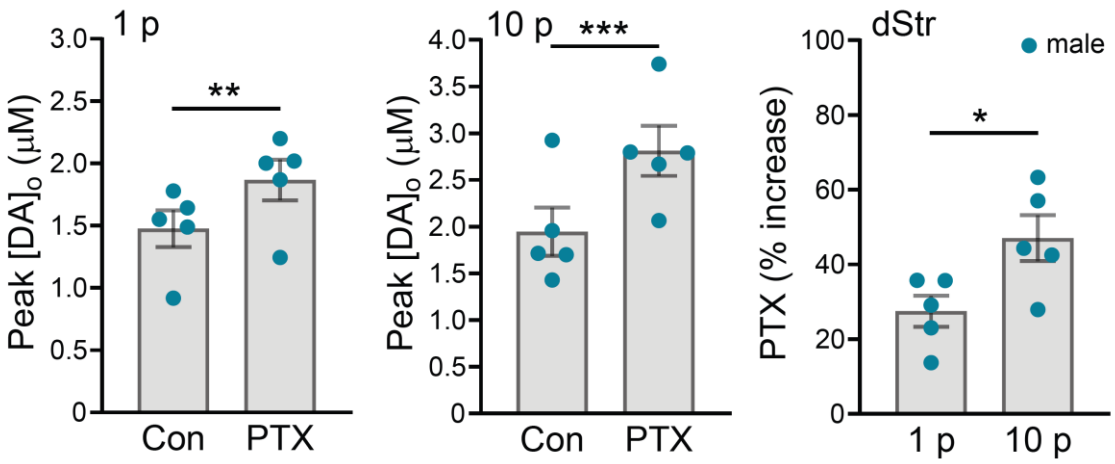

Figure S6. Greater amplification of DA release by PTX on 10 p than on 1 p occurs at near physiological temperatures (Related to Main Figures 2, 3 and 4).

Effect of the $GABA_AR$ Cl^- channel blocker picrotoxin (PTX, 100 μM) on peak $[DA]_o$ evoked by 1 p and 10 p optical stimulation of DA axons using multisite protocol at 30-32˚C in the dStr of males (blue circles). PTX significantly amplified DA release by 1 p (left panel) and 10 p (middle panel) (**p < 0.01, ***p < 0.001 paired t-test, n = 5 mice) indicating that regulation of DA release by ambient GABA acting at DA axonal $GABA_ARs$ persists at near physiological temperatures and that enhanced transporter activity does not impede autoregulation of DA release by GABA corelease. Right panel: PTX had a significantly greater enhancing effect on peak $[DA]_o$ evoked by phasic stimuli (10 p) *versus* tonic stimuli (1 p) (*p < 0.05, n = 5). Data are mean ± SEM.

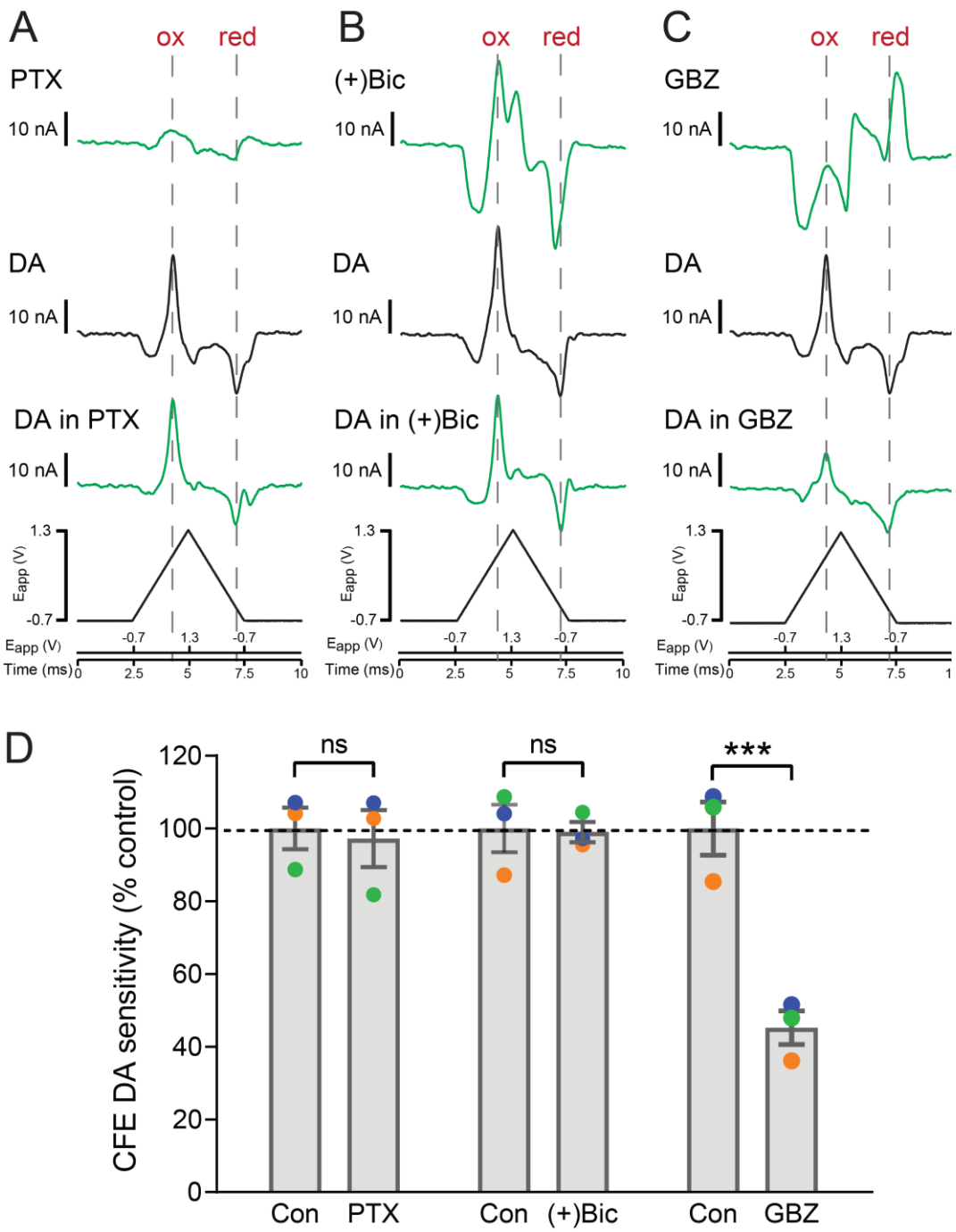

Figure S7. Electroactivity and effect on electrode sensitivity to DA of commonly used $GABA_AR$ antagonists using FSCV at carbon fiber electrodes (Related to Main Figures 2, 3, 4 and 5).

(A) Upper panel, Faradaic current *versus* time plot showing that picrotoxin (PTX, 100 µM) alone did not exhibit electroactivity in the range of the voltage waveform used for DA detection (lower

panel), nor did it alter the sensitivity of the carbon fiber microelectrode (CFM) to DA (1 µM) (middle panel).

(B) (+)Bicuculline ((+)Bic, 10 µM) displayed marked electroactivity when applied alone, as seen in the large oxidation and reduction peaks that occurred at similar potentials to that of DA, as well as an smaller oxidation peak close to the switch potential (upper panel). However, no change in CFM sensitivity to DA was seen with (+)Bic (middle panel). **(C)** Gabazine (GBZ, 10 µM) alone induced complex changes in the Faradaic current (upper panel). Moreover, GBZ caused a profound decrease in the sensitivity of the CFM to DA. (D) Graph showing average data obtained from three different CFMs to DA in the absence and presence of each $GABA_AR$ antagonist, with each CFM tested three times.

ns = non-significant; $p > 0.05$; ***$p < 0.001$ *versus* respective control in DA alone. Data are mean ± SEM.

Supplemental References

S1. Saunders, A., Macosko, E.Z., Wysoker, A., Goldman, M., Krienen, F.M., de Rivera, H., Bein, E., Baum, M., Bortolin, L., Wang, S., Goeva, A., Nemesh, J., Kamitaki, N., Brumbaugh, S., Kulp, D., and McCarroll, S.A. (2018) Molecular diversity and specializations among the cells of the adult mouse brain. Cell *174*, 1015-1030.

S2. Carmichael, K., Sullivan, B., Lopez, E., Sun, L., and Cai, H. (2021) Diverse midbrain dopaminergic neuron subtypes and implications for complex clinical symptoms of Parkinson's disease. Ageing Neurodegen. Dis. *1*, 10.20517/and.2021.07.

S3. Pereira Luppi, M., Azcorra, M., Caronia-Brown, G., Poulin, J.F., Gaertner, Z., Gatica, S., Moreno-Ramos, O.A., Nouri, N., Dubois, M., Ma, Y.C., Ramakrishnan, C., Fenno, L., Kim, Y.S., Deisseroth, K., Cicchetti, F., Dombeck, D.A., and Awatramani, R. (2021) Sox6 expression distinguishes dorsally and ventrally biased dopamine neurons in the substantia nigra with distinctive properties and embryonic origins. Cell Rep. *37*, 109975.